LONG-LASTING DIFFUSIVE SOLUTIONS FOR SYSTEMS OF CONSERVATION LAWS *

Arthur Azevedo **Dan Marchesin**
Bradley J. Plohr **Kevin Zumbrun**

Abstract

We investigate long-lasting solutions of two-component systems of conservation laws. These solutions arise from quasi-Riemann problems, which are perturbations of Riemann initial-value problems for the conservation laws augmented by a small parabolic term. Our study focuses on solutions containing a sequence of waves with the same speed, each wave having a viscous profile that is a saddle-saddle connection. Particular examples arise from homoclinic cycles, 2-cycles of shock waves, and 3-cycles of shock waves. Such wave sequences collapse in the large-time limit, but can survive for long time periods if the viscosity is small. This phenomenon sheds light on the ill-posedness of the problem of finding time-asymptotic solutions and on the related occurrence of Riemann problems that have multiple solutions. Moreover, long-lasting solutions depend continuously on the initial data; they therefore provide a global picture of quasi-Riemann solutions as a continuum even when the corresponding Riemann solutions do not depend continuously on the data.

Resumo

Neste trabalho investigamos soluções de longa duração em sistemas de duas leis de conservação. Tais soluções surgem em problemas "quase" Riemann, que são perturbações de problemas de Riemann através da introdução de termos parabólicos (termos de viscosidade) pequenos. Nosso estudo focaliza soluções que contêm uma seqüência de ondas de mesma velocidade, onde cada onda tem um perfil viscoso que é uma ligação entre

**Key words and phrases.* conservation law, Riemann problem, quasi-Riemann problems, long-lasting waves.
This work was supported in part by: CAPES under Grant BEX0012/97-1; FEMAT under Grant 990003; CNPq under Grant CNPq/NSF 910029/95-4; CNPq under Grant 520725/95-6; CNPq under Grant 300204/83-3; MCT under Grant PCI 650009/97-5; FAPERJ under Grant E-26/150.936/99; FINEP under Grant 77970315-00; CNPq under Grant 301411/95-6; NSF under Grant DMS-9732876; DOE under Grant DE-FG02-90ER25084; ONR under Grant N00014-94-1-0456; and NSF under Grants DMS-9107990 and DMS-9706842.

duas selas. Exemplos particulares surgem a partir de ciclos homoclínicos, de 2-ciclos e de 3-ciclos. Tais seqüências de ondas desaparecem quando o tempo tende para infinito mas podem sobreviver por longos períodos, se o termo de viscosidade for pequeno. Este fenômeno esclarece o comportamento mal posto encontrado no estudo de soluções assintóticas e o aparecimento de certas soluções múltiplas encontradas em problemas de Riemann. Além disso, soluções de longa duração dependem continuamente dos dados iniciais; elas ajudam na compreensão da estrutura global contínua de soluções "quase" Riemann, mesmo quando as soluções de Riemann correspondentes não dependem continuamente dos dados iniciais.

1. Introduction

Nonlinear systems of conservation laws have discontinuous (weak) solutions known as shock waves. In the absence of restricting criteria, weak solutions are not uniquely determined by the initial data. Since Courant-Friedrichs [12] and Gel'fand [18], the remedy for such nonuniqueness has been to regard each individual shock wave as admissible if it is the small-viscosity limit of a traveling wave solution of the conservation laws augmented by parabolic terms dictated by the physics.

However, solutions generally contain several waves. In this paper, we investigate situations where *wave sequences* are small-viscosity limits of solutions of the parabolic system for appropriate initial data. As we will see, the *effect of viscosity on a wave sequence cannot be reduced to the combined effects of viscosity on each individual wave.*

Consider a solution of the parabolic system containing a sequence of waves. When isolated, each wave in the sequence gives rise to a time-asymptotic limiting solution. The wave sequence itself, however, might not survive in the large-time limit because its component waves can interact with each other and lose their individualities. Nevertheless, if the viscosity is small, a wave sequence can last for a long time. The life span increases as viscosity decreases.

In this paper we investigate *long-lasting solutions* of the parabolic two-component system

$$U_t + F(U)_x = \epsilon\,[B(U)U_x]_x\,. \tag{1.1}$$

We focus attention on initial data with a special form:

$$U(x,0) = \begin{cases} U_l & \text{for} \quad x < -\epsilon, \\ \bar{U}(x/\epsilon) & \text{for} \quad -\epsilon \le x \le \epsilon, \\ U_r & \text{for} \quad \epsilon < x. \end{cases} \tag{1.2}$$

Here ϵ is a small positive number, U_l and U_r are constant states, and $\bar{U}$ is continuous on the interval $[-1,1]$ and such that $\bar{U}(-1) = U_l$ and $\bar{U}(1) = U_r$. We call such an initial-value problem a *quasi-Riemann problem.* Inspired by the theory of systems of conservation laws, we expect solutions to comprise sequences of approximate rarefaction waves and approximate traveling waves with non-decreasing speeds from left to right. (Notice that we allow adjacent waves to have the same speed, even though we regard the waves as distinct.)

Approximate traveling waves should tend to shock waves in the limit as $\epsilon \to 0^+$. In addition to Lax shock waves of family 1 and family 2, for which the traveling wave orbit connects a saddle point and a node, there exist shock waves with saddle-saddle connecting orbits. We distinguish two kinds of saddle-saddle waves: *transitional waves*, for which the left state U_- is a saddle point, the right state $U_+ \neq U_-$ is also a saddle point, and a heteroclinic orbit connects them; and *homoclinic waves*, for which the left and right states coincide and the orbit connects this saddle point to itself. The existence of transitional and homoclinic waves allows adjacent shock waves to have the same speed. (The Lax characteristic criterion precludes the possibility.) Thus there is a new phenomenon: sequences of transitional waves with the same speed separated by constant states.

Such sequences lie at the root of nonuniqueness of solutions of Riemann problems for the inviscid conservation laws [2, 3]. The occurrence of multiple solutions implies the ill-posedness for the following problem: given only the states U_l and U_r, find the time-asymptotic solution of the quasi-Riemann problem. Of course, a solution for the parabolic system is uniquely determined by its initial data; even when the solution is not determined by U_l and U_r, by themselves, it is determined by specifying extra information, namely how $\bar{U}$ interpolates between U_l and U_r. On the other hand, in the limit as $\epsilon \to 0^+$, different choices of $\bar{U}$ can converge to different solutions of the inviscid Riemann problem.

By studying the corresponding quasi-Riemann solutions, we can also understand why Riemann problems with multiple solutions can fail to be continuous in the initial data: as explained in [4], the anomalous behavior is related to the collapse of distinct quasi-Riemann solutions in the limit as $\epsilon \to 0^+$.

In previous work [5], we studied the nonuniqueness of Riemann solutions arising from 2-cycles of shock waves. We noticed the important role played by solutions containing solitary waves, which, as $\epsilon \to 0^+$, become indistinguishable from a constant state. Although these homoclinic solutions are not stable, they can be made to last a long time in numerical experiments by choosing $\bar{U}$ near to a codimension-one manifold in the space of initial data. This example served to motivate the present investigation.

In this paper, after setting up notations in Section 2, we describe three types of long-lasting solutions: stable ("Riemann") solutions in Section 3, unstable (homoclinic) solutions in Section 4, and metastable solutions (sequences of several transitional waves with identical, or almost identical, speeds) in Section 5. We discuss further our results in Section 6. In Appendix A, we show that 3-cycles exist for quadratic models. Bifurcations of 3-cycles, which we discuss in Appendix B, generate the examples presented in Section 5.

2. Preliminaries

In this paper, we assume that system (1.1) is a two-component system, so that $U = (u, v)^T$. We assume that the eigenvalues $\lambda_i(U)$ $(i = 1, 2)$ of $F'(U)$ are real and distinct except in a compact region.

Rarefaction waves are associated to the eigenvectors of $F'(U)$. More precisely, if $r_i(U)$ is a right eigenvector of $F'(U)$ associated to the eigenvalue $\lambda_i(U)$, then a rarefaction wave $U(\zeta)$ of family i from U_- to U_+ satisfies

$$\begin{array}{l} \frac{dU(\zeta)}{d\zeta} = r_i(U(\zeta)), \\ U(\zeta_1) = U_-, U(\zeta_2) = U_+, \text{ with } \zeta_1 < \zeta_2. \end{array} \tag{2.1}$$

Here $\zeta = x/t$ and $r_i(U)$ is chosen so that $\lambda_i'(U)\, r_i(U) = 1$.

A traveling wave $U(\xi)$ is a solution of the system of ordinary differential equations

$$\dot{U} = B(U)^{-1} \{-s\,[U - U_-] + F(U) - F(U_-)\} \tag{2.2}$$

satisfying $\lim_{\xi\to\pm\infty} U(\xi) = U_\pm$. Here $\xi = x - st$, with s being the propagation speed.

Strictly speaking, the equilibria U_- and U_+ are attained only in the limits $\lim_{x\to\pm\infty} U(\xi) = U_\pm$. However, as the rate of approach is exponentially fast, approximate solutions of the parabolic system can be obtained by juxtaposing traveling waves, so long as the propagation speeds are in proper order. In this situation, the equilibria serve as constant states appearing in the wave sequence.

Admissible Lax shock waves of family 1 are associated to an orbit leading from a repeller node or spiral U_- to a saddle point U_+, whereas admissible Lax shocks of family 2 are associated to an orbit from a saddle U_- to an attracting node or spiral U_+.

Transitional and homoclinic waves are associated to saddle-saddle connections. Using saddle-saddle connections, we can define a map T. Let γ denote the orbit connecting the two saddles. Then T associates the α-limit saddle of γ to its ω-limit saddle. In other words, $U_2 = T(U_1)$, where $U_1 = \alpha(\gamma)$ and $U_2 = \omega(\gamma)$. (Here U_1 and U_2 play the role of U_- and U_+, respectively, in Eq. (2.2).) We call this map the *transitional map.*

Compositions of transitional maps may give rise to *cycles.* For example, homoclinic-cycles are $U^* = U_1^* = U_2^* = T(U_1^*)$ (Fig. 2.), 2-cycles are $U_1^* = T_2(U_2^*)$, where $U_2^* = T_1(U_1^*) \neq U_1^*$ (Fig. 2.), 3-cycles are $U_1^* = T_3(U_3^*), U_3^* = T_2(U_2^*), U_2^* = T_1(U_1^*)$, where $U_i^* \neq U_j^*$ $(i \neq j)$ (Fig. 2.). Viewed as transitional shocks, all the waves in such cycles necessarily have the same speed (evidently, in the case of 2-cycle, by the triple shock rule in the case of 3-cycle, see Appendices below).

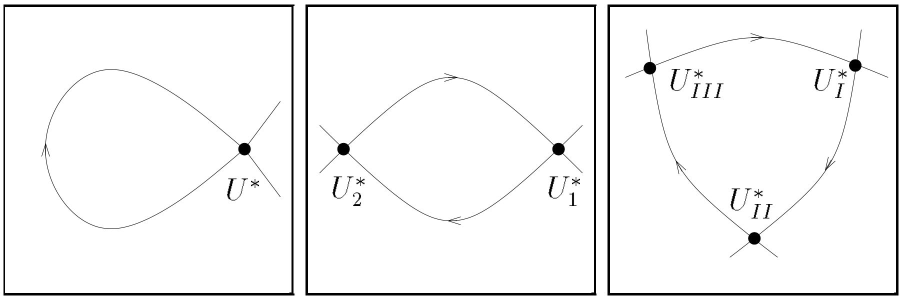

(a) Homoclinic-cycle (b) 2-cycle (c) 3-cycle

Figure 2.1: Polycycles of shock waves.

Composing i-rarefactions and i-shocks ($i = 1, 2$) with increasing speed we obtain an i-wave group (or i-wave), which we denote by W_i.

We adopt the same notation T for transitional map and for transitional shock, whenever there is no risk of confusion. We also use the notation $L \xrightarrow{W} R$ to indicate that the state L is connected to the state R by a wave W (W may be a 1-wave (W_1), a 2-wave (W_2), or a transitional wave (T)).

To describe the solutions, we consider two types of initial data: local, when U_l and U_r are close to a state U_a, and non-local, when U_l lies in a neighborhood of a state U_b and U_r lies in a neighborhood of a state U_c, such that U_b does not coincide with U_c and $U_c = T(U_b)$.

3. Stable Solutions

For local initial data, the Riemann and quasi-Riemann solutions are $U_l \xrightarrow{W_1} U_{a'} \xrightarrow{W_2} U_r$, where $U_{a'}$ lies in a neighborhood of U_a. The Riemann solution is the classical Lax solution. Fig. 3. shows the quasi-Riemann solution in the uv-plane and Fig. 3. shows it in the xu-plane.

For non-local initial data, an example of a Riemann solution is $U_l \xrightarrow{W_1} U_{b'} \xrightarrow{T} U_{c'} \xrightarrow{W_2} U_r$, where $U_{b'}$ lies in a neighborhood of U_b and $U_{c'}$ lies in a

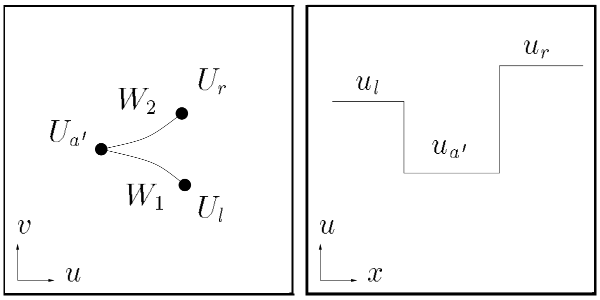

(a) Local solution (b) Local solution

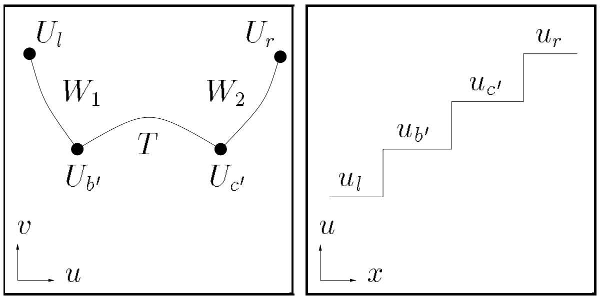

(c) Non-local solution (d) Non-local solution

Figure 3.1: Riemann solutions.

neighborhood of U_c. Fig. 3. shows this solution in the uv-plane and Fig. 3. shows it in the xu-plane.

For non-local initial data, one Riemann and quasi-Riemann solutions are $U_l \xrightarrow{W_1} U_{b'} \xrightarrow{T} U_{c'} \xrightarrow{W_2} U_r$, where $U_{b'}$ lies in a neighborhood of U_b and $U_{c'}$ lies in a neighborhood of U_c. Fig. 3. shows the quasi-Riemann solution in the uv-plane and Fig. 3. shows it in the xu-plane.

4. Unstable Solutions Associated to Homoclinic Orbits

Homoclinic solutions were introduced in [3]. They can be obtained from a constant state $U^* = (u^*, v^*)$ and a fixed speed s^* such that U^* is a saddle point of (2.2) connected to itself by a homoclinic orbit. More precisely, a homoclinic solution is a quasi-Riemann solution which contains an intermediate state U^* connected to itself by a single wave.

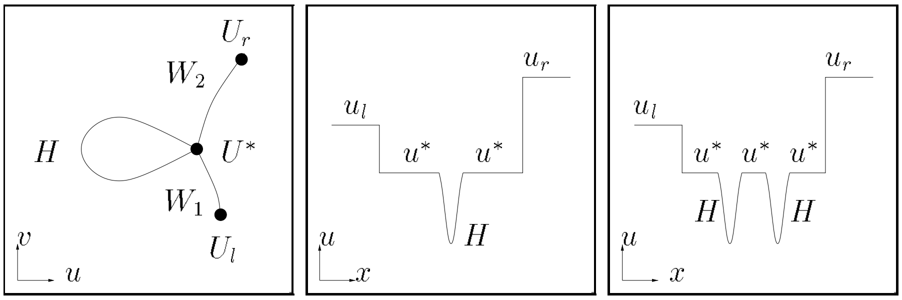

(a) Solution drawn in the uv-plane

(b) 1 loop

(c) 2 loops

Figure 4.1: Homoclinic solutions.

A simple homoclinic solution can be obtained from a classical Riemann solution when U^* coincides with $U_{a'}$: $U_l \xrightarrow{W_1} U^* \xrightarrow{H} U^* \xrightarrow{W_2} U_r$, where H represents the homoclinic shock. Fig. 4. shows an example of such a solution in the uv-plane and Fig. 4. and Fig. 4. shows it in the xu-plane. As one can easily check, there is no difference in the uv-plane between a quasi-Riemann solution containing 1 loop or 2 loops. Once a homoclinic orbit appears in the solution, one can use many loops to construct different solutions. Fig. 4. and present examples showing the first coordinate u of homoclinic solutions containing one loop and two loops, respectively.

The homoclinic solutions considered exist only for local initial data. Numerical experiments so far indicate that homoclinic solutions are unstable. Analytic proof for some cases can be found in [17]. We conjecture that these solutions have behavior similar to unstable singularities in dynamical systems. However, we call these solutions long-lasting because for initial data chosen near a codimension-one manifold they are long-lasting.

Despite the fact that these solutions are unstable, they are necessary to understand the topological behavior of the solution manifold associated to the problem [4].

5. Metastable Solutions

For solutions containing 2-cycles and 3-cycles we can consider local and non-local initial data. Since the technique to construct the solution for the local case is the same for both type of cycles, we present only the local 2-cycle case. Similarly, since the techniques to construct the non-local 2-cycle and 3-cycle are analogous, we present here only a non-local 3-cycle case. The other cases can be easily obtained by analogy with these two cases.

5.1. Solutions associated to 2-cycle for local data. Without loss of generality, we consider states U_l and U_r in a neighborhood of the same saddle U_1^* (Fig. 5.). This case was initially studied in [5].

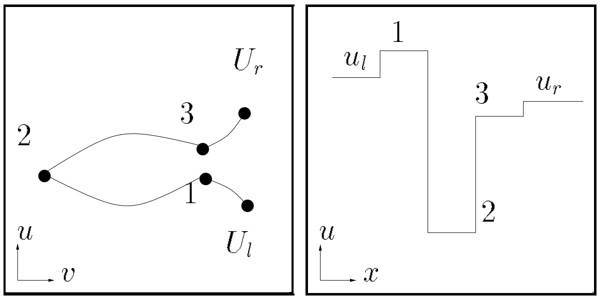

(a) 1 loop (b) 1 loop

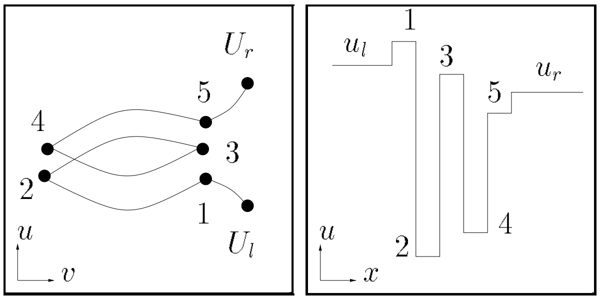

(c) 2 loops (d) 2 loops

Figure 5.1: Perturbed 2-cycle solutions for certain local initial data.

We first consider the case in which $U_{a'}$ coincides with U_1^*. In this case, one of the quasi-Riemann solution consists of $U_l \xrightarrow{W_1} U_1^* \xrightarrow{T_1} U_2^* \xrightarrow{T_2} U_1^* \xrightarrow{W_2} U_r$. Depending on the loop cycle present, by perturbing the data it may be possible to obtain quasi-Riemann solutions containing many such loops.

Now we consider a perturbation of U_l and U_r such that $U_{a'}$ still lies in a neighborhood of U_1^*. It is possible to construct the solution $U_l \xrightarrow{W_1} 1 \xrightarrow{T_1} 2 \xrightarrow{T_2} 3 \xrightarrow{W_2} U_r$, where the state indicated by $i+1$ is obtained from the state indicated by i through the mapping T_i ($i = 1, 2$ and T_i are transitional maps). Fig. 5. shows this solution in the uv-plane and Fig. 5. shows it in the xu-plane.

Moreover, for *certain models*, and certain classes of perturbation in the initial data, one can obtain the solution $U_l \xrightarrow{W_1} 1 \xrightarrow{T_1} 2 \xrightarrow{T_2} 3 \xrightarrow{T_3} 4 \xrightarrow{T_4} 5 \xrightarrow{W_2} U_r$. Fig. 5. shows this solution in the uv-plane and Fig. 5. shows it in the xu-plane.

Remark. The existence of such solutions is implicit from the proof of Theorem 4.2 in [5] for certain models (see the final sentence of the statement of the theorem).

5.2. Solutions associated to 3-cycles for non-local data. We first consider the non-local case in which U_b coincides with U_{III}^* and U_c coincides with U_I^* (Fig. 5.). For this data, one of the quasi-Riemann solutions is $U_l \xrightarrow{W_1} U_{III}^* \xrightarrow{T_1} U_I^* \xrightarrow{T_2} U_{II}^* \xrightarrow{T_3} U_{III}^* \xrightarrow{T_1} U_I^* \xrightarrow{W_2} U_r$. Again, examples show that for *certain models* and certain class of initial data, one can obtain instead solutions with many loops. Such examples were obtained numerically with a high resolution code for solving parabolic equations (EVOLVE) and confirmed with our code for wave structure analysis (RP).

Considering certain classes of perturbations of above data containing certain 3-cycles, we can obtain long lasting solutions $U_l \xrightarrow{W_1} 1 \xrightarrow{T_1} 2 \xrightarrow{T_2} 3 \xrightarrow{T_3} 4 \xrightarrow{T_4} 5 \xrightarrow{W_2} U_r$, where the state indicated by $i+1$ is obtained from the state indicated by i through the transitional mapping T_i ($i = 1, \ldots, 4$). Fig. 5. shows this solution in the uv-plane and Fig. 5. shows it in the xu-plane. Again, since a loop is present, other solutions containing many such loops are often allowed.

For other classes of perturbations, the quasi-Riemann solution is $U_l \xrightarrow{W_1}$

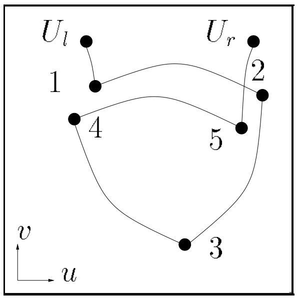

(a) 1 loop

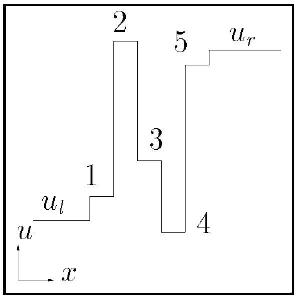

(b) 1 loop

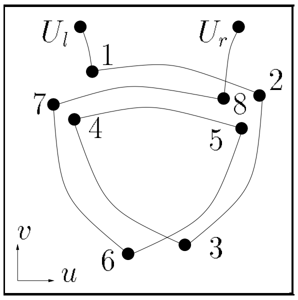

(c) 2 loops

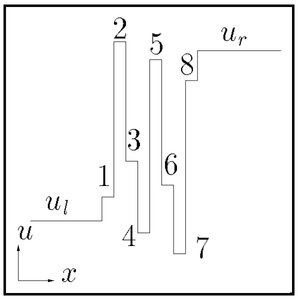

(d) 2 loops

Figure 5.2: Perturbed 3-cycles solutions for certain non-local initial data.

$1 \xrightarrow{T_1} 2 \xrightarrow{T_2} 3 \xrightarrow{T_3} 4 \xrightarrow{T_4} 5 \xrightarrow{T_5} 6 \xrightarrow{T_6} 7 \xrightarrow{T_7} 8 \xrightarrow{W_2} U_r$. Fig. 5. shows this solution in the uv-plane and Fig. 5. shows it in the xu-plane.

6. Discussion

The study of long-lasting solutions exemplifies how, in understanding the global behavior of solutions of systems of conservation laws, it is fundamental to account for the effect of the associated parabolic terms, not only on individual waves, but also on sequences of waves. For example, in a solution arising from a 2-cycle, each of the two transitional waves might be stable even though their combination is not stable. On the other hand, the combination can be long-lasting, or metastable, because it takes a long time before the two waves interact and lose their individualities. An interesting open problem is to understand precisely the asymptotic behavior of these solutions.

We conjecture that the oscillatory waves detected by Frid-Liu [16] and Canic-Peters [9] are related to the multiple-loop solutions presented here. Specifically, we conjecture (based on numerical experiment, to be reported elsewhere) that oscillatory waves arise as pieces of quasi-Riemann solutions generated by linearly unstable middle states. Understanding this behavior is an interesting open problem.

Remark. Our joint work on multiloop solutions and the existence of 2- and 3-cycles was presented in preliminary form in the talk of D. Marchesin at the Fifth International Conference on Hyperbolic Problems (1994) in Stony Brook, but it was not included in the proceedings paper [6]. This work, along with the conjectured relationship between global (3-cycle) structure and oscillatory waves, was discussed in the talk of K. Zumbrun at the Sixth International Conference on Hyperbolic Problems (1996) in Hong Kong. The material presented in the Appendices is taken from an unpublished manuscript prepared at the same time as Ref. [7].

Appendices: Global Structure for Quadratic Flux Models

In these appendices, we investigate further the class of two-component models (1.1) with quadratic flux $F(U)$ and constant viscosity matrix B, employed to obtain the examples of waves discussed in this paper. These models, though rather general, have sufficient extra structure to allow a complete analysis. Referring to the classification scheme of Wenstrom (née Hurley) [21, 27] (similar to that of Schaeffer and Shearer [24] for homogeneous quadratic flux models), we point out that for type I_B models similar to those studied in Ref. [16], both 2- and 3-cycles generically occur. Moreover, we carry out a global bifurcation, identifying large-scale structures which may be of use in future analytic study of the formation of numerically observed oscillatory patterns. The main tool in our analysis is the observation of Ref. [22] that a large class of transitional shocks have straight line profiles which can be calculated explicitly. (In particular, one of the connections in a 2-cycle must always be such a straight line connection [17]).

Appendix A. Existence of 2- and 3-Cycles in Quadratic Flux Models

In [7], it was shown that the 2-cycle configuration discussed in Section 5.1 appears generically in quadratic flux models of type I_B–II_B in the classification scheme of Wenstrom [21, 27], in particular for those that are typically studied with relation to multiphase flow [24]. This follows as a corollary of the existence for all type models of special DRS bifurcation points. In this section, we prove an analogous result regarding appearance of 3-cycle configurations discussed in Section 5.2: namely, we first prove the existence for generic quadratic models of a special triple shock configuration; from this, we can conclude the generic existence of a (unique) 3-cycle for models of (and only of) type I_B. This furnishes a rich set of examples for the discussion in the main body of the paper.

A.1. Existence of 3-cycles in quadratic flux models. We seek distinct states U_1, U_2, and U_3 which are pairwise joined by straight-line connections. Let the angles of the directions of the connections be denoted ϕ_1, ϕ_2, and ϕ_3; thus

$$(-\sin\phi_3, \cos\phi_3)\,(U_2 - U_1) = 0, \tag{A.1}$$

$$(-\sin\phi_1, \cos\phi_1)\,(U_3 - U_2) = 0, \tag{A.2}$$

$$(-\sin\phi_2, \cos\phi_2)\,(U_1 - U_3) = 0. \tag{A.3}$$

A necessary and sufficient condition [22] to have a straight-line connection joining these points is that $\mu_B(\phi_j) = 0, \quad j = 1, 2, 3,$ where

$$\mu_B(\phi) = (-\sin\phi, \cos\phi)B^{-1}F''(0) \cdot \begin{pmatrix} \cos\phi \\ \sin\phi \end{pmatrix}^2 \tag{A.4}$$

and $\tilde{\mu}_B(\phi_j) \neq 0, \quad j = 1, 2, 3,$ where

$$\tilde{\mu}_B(\phi) = (\cos\phi, \sin\phi)B^{-1}F''(0) \cdot \begin{pmatrix} \cos\phi \\ \sin\phi \end{pmatrix}^2. \tag{A.5}$$

Notice that μ_B is a homogeneous cubic polynomial in $(\cos\phi, \sin\phi)$; we assume that it has three distinct roots.

Since the flux F is quadratic, the Rankine-Hugoniot conditions for the shock wave from U_1 to U_2 can be written

$$\left[F'(\frac{U_1+U_2}{2}) - sI\right](U_2 - U_1) = 0. \tag{A.6}$$

Multiplying this equation by $(-\sin\phi_3, \cos\phi_3)$ eliminates the shock speed s:

$$(-\sin\phi_3, \cos\phi_3)F'(\frac{U_1+U_2}{2})(U_2 - U_1) = 0. \tag{A.7}$$

Following Ref. [22], we define the coefficient functions α, β, and γ by

$$(-\sin\phi, \cos\phi)F'(\bar{U})\begin{pmatrix}\cos\phi\\ \sin\phi\end{pmatrix} = \alpha(\phi)\bar{u} + \beta(\phi)\bar{v} + \gamma(\phi), \tag{A.8}$$

for any $\bar{U} = (\bar{u}, \bar{v})$. Thus A.7 becomes

$$\alpha(\phi_3)(\frac{u_1+u_2}{2}) + \beta(\phi_3)(\frac{v_1+v_2}{2}) + \gamma(\phi_3) = 0. \tag{A.9}$$

Similarly,

$$\alpha(\phi_1)(\frac{u_2+u_3}{2}) + \beta(\phi_1)(\frac{v_2+v_3}{2}) + \gamma(\phi_1) = 0, \tag{A.10}$$

$$\alpha(\phi_2)(\frac{u_3+u_1}{2}) + \beta(\phi_2)(\frac{v_3+v_1}{2}) + \gamma(\phi_2) = 0. \tag{A.11}$$

Let

$$A_{j,\pm} = \begin{pmatrix}\alpha(\phi_j) & \beta(\phi_j)\\ \mp\sin\phi_j & \pm\cos\phi_j\end{pmatrix}, \quad R_j = \begin{pmatrix}-2\gamma(\phi_j)\\ 0\end{pmatrix}. \tag{A.12}$$

Then the linear system (A.1), (A.2), (A.3), (A.9), (A.10), (A.11) can be written

$$\begin{pmatrix}A_{2,-} & 0 & A_{2,+}\\ 0 & A_{1,+} & A_{1,-}\\ A_{3,+} & A_{3,-} & 0\end{pmatrix}\begin{pmatrix}U_1\\ U_2\\ U_3\end{pmatrix} = \begin{pmatrix}R_2\\ R_1\\ R_3\end{pmatrix}. \tag{A.13}$$

It is easy to check that this system has full row rank unless $(\alpha(\phi_j), \beta(\phi_j)) = (0,0)$ for $j = 1$, 2, or 3. Otherwise, this system can be solved for U_1, U_2, and U_3.

The states U_1, U_2, and U_3 are either all distinct or all coincident. For, $U_1 = U_2$, by (A.2)–(A.3), implies that $U_3 - U_1$ is orthogonal to both $(-\sin\phi_1, \cos\phi_1)$

and $(-\sin\phi_2, \cos\phi_2)$, which in turn implies that $U_3 = U_1 (= U_2)$. If they coincide, *i.e.*, there is a common point satisfying (A.9)–(A.11), then this point lies on the three *viscosity lines* defined by

$$\alpha(\phi_j)u + \beta(\phi_j)v + \gamma(\phi_j) = 0, \quad j = 1, 2, 3. \tag{A.14}$$

Theorem A.1. *Let F, B be such that $(\alpha(\phi), \beta(\phi)) \neq 0$ for all ϕ. Then, there exist three distinct states U_j joined by straight-line connections if and only if the following conditions hold:*

- *(i) There exist three* viscosity angles *ϕ_j satisfying $\mu_B(\phi_j) = 0$ which are distinct (mod π);*
- *(ii) For $j = 1, 2, 3$, $\tilde{\mu}_B(\phi_j) \neq 0$;*
- *(iii) The viscosity lines $\alpha(\phi_j)u + \beta(\phi_j)v + \gamma(\phi_j) = 0$, $j = 1, 2, 3$, do not have a common intersection point.*

Proof: Assume that there exist straight-line connections between distinct U_j. Since connections occur only at viscosity angles, the angles of the sides of the triangle formed by the U_j represent three distinct viscosity angles ϕ_j. Recall, further, that connections exist only if $\tilde{\mu}_B(\phi_j) \neq 0$. Because the viscosity angles are distinct and $(\alpha(\phi_j), \beta(\phi_j)) \neq 0$ by assumption, the solution (U_1, U_2, U_3) of system (A.13) is unique. If the viscosity lines were to meet at a point U^*, then (U^*, U^*, U^*) would be a solution as well, a contradiction. For, (A.1)–(A.3) are satisfied trivially for any triple (U, U, U), while (A.9)–(A.11) would be satisfied by the definition of viscosity line. Thus we obtain (i)–(iii).

On the other hand, suppose that (i)–(iii) hold. Since the viscosity angles are distinct, and $(\alpha(\phi_j), \beta(\phi_j)) \neq 0$, system (A.13) has a unique solution (U_1, U_2, U_3). If any two of these coincide, then they all do, so by (A.9)–(A.11) the three viscosity lines have a common intersection, a contradiction. Thus there exist three distinct states U_j joined by straight-line connections.

□

Remark. Condition (iii) has a straightforward interpretation in terms of conservation laws. Each viscosity line is tangent to the conic section that constitutes the boundary of the region of nonstrict hyperbolicity [22, App. B.1]. When the nonstrictly hyperbolic region is bounded, therefore, it is contained in the triangle formed by the intersection of the viscosity lines. If this triangle degenerates to a point, then the nonstrictly hyperbolic region must likewise consist of a single, umbilic point. In fact, it is true for any conic section (indeed, this follows from the bounded case, by extension) that if three distinct tangent lines meet at a point then the conic section is itself a point. Thus if the viscosity lines are distinct, then (iii) is equivalent to the condition that the nonhyperbolic region for the model does not consist of a single point.

Theorem A.1 shows that, except for a set of measure zero in the space of model parameters, every quadratic model having three distinct viscosity angles has a unique triple shock configuration. Recall ([21, 27] or [7, Section 4]) that models in Cases I_B–III_B in the classification scheme of Wenstrom have three viscosity angles, whereas those in Case IV_B have none. Thus, the triple shock configuration occurs in all cases except for Case IV_B.

The triple shock is a triple cycle if and only if all three vertices are saddles, which further restricts to Case I_B. (Alternatively, the three viscosity angles must be "active", see discussion [7], Section 4). That is: *Except for a set of measure zero in the space of model parameters, there exists a triple cycle precisely in Case I_B.*

A.2. Associated phase portrait. A three cycle connection is quite special in a planar quadratic ODE. It is not difficult, using the methods of Ref. [10, 11], to show that each of the connecting orbits must lie along straight lines. For, the flow must be transverse to any side of the triangle of vertices which is not an orbit, and this side would divide the interior of the 3-cycle into two invariant regions, in backward and forward time. These would each therefore contain a rest point, making five rest points in all, a contradiction of the fact that quadratic ODE have only four rest points. Moreover, it can be shown, by affine reduction to canonical form, that the ODE must be quasi-Hamiltonian in the sense that there is a first integral H preserved along orbits [8]. Thus there is an infinite family of periodic orbits in the interior of the 3-cycle.

Appendix B. Global Bifurcation of DRS and 3-Cycle Configurations

In [7], the bifurcation of special DRS points was investigated; three rest points collide in the phase portrait of the traveling wave ODE. Under suitable nondegeneracy hypotheses, it was shown that these exhibit the three-parameter bifurcation described by Dumortier *et al.* [13]. In particular, for DRS points of *saddle type*, for which the colliding rest points consist of two saddles and a node, this bifurcation includes the emergence of precisely two double-saddle cycle (2-cycle) curves, corresponding to the two rest points in the cycle. (It also includes homoclinic loops, limit cycles, and a variety of other behaviors, see [5, 13]). Here, we show an analogous result for the bifurcation of the triple cycle configuration, namely that from each vertex of the 3-cycle there emerge precisely two double-saddle curves, featuring straight-line and curved connections leaving from the vertex in question. That is, both codimension three bifurcations feature the appearance of double-saddle cycles. We go on to show, under a strong nondegeneracy hypothesis, that, for type I_B models, this is the only way that 2-cycles arise; indeed, the two-saddle cycle curves connect the three vertices of the 3-cycle to the three DRS points found in type I_B models (see [7], for counting of DRS points). This picture is also what we see numerically.

B.1. Bifurcation of the 3-cycle. The bifurcation of the 3-cycle is similar to that of the 2-cycle [14]. We describe those aspects relevant to the present study, indicating the main features of their proof. For other aspects of the bifurcation of quadratic 3-cycles, see Ref. [28] or [23].

Let $\Gamma_{1,2}$, $\Gamma_{2,3}$, and $\Gamma_{3,1}$ be straight-line saddle-saddle connections joining the pairs (U_1^*, U_2^*), (U_2^*, U_3^*), and (U_3^*, U_1^*), respectively, with common speed s^*, and define $U_j(U_-, s)$ to be the rest point of system (2.2) near U_j^* associated with parameters (U_-, s). We use a cyclic indexing system, $j = j(\mathrm{mod}3)$. Choose lines $L_{j,j+1}$ transverse to the $\Gamma_{j,j+1}$ and orient them as indicated in Fig. B.. Take the origin on the transversal $L_{j,j+1}$ to be the point where the stable manifold of U_j meets it; then the unstable manifold of U_{j+1} meets this transversal at the point $d_{j,j+1}(U_-, s)$. The *separation functions* $d_{j,j+1}$ are smooth, and their derivatives at (U_-, s) can be expressed as Melnikov integrals [20]. We make the nondegeneracy assumption that these derivatives are full rank, *i.e.*, the map from (U_-, s) to $(d_{1,2}, d_{2,3}, d_{3,1})$ is locally invertible. In the standard way, we can thus replace (U_-, s) by the more convenient bifurcation parameters $(d_{1,2}, d_{2,3}, d_{3,1})$. In these coordinates, the 2-surfaces $d_{j,j+1} = 0$ correspond to straight-line saddle-saddle connections from U_j to U_{j+1}.

Curved connections: Let $\mu_j^- < 0 < \mu_j^+$ denote the eigenvalues at the equilibria U_j^* for (U_-^*, s^*) of Eq. (2.2), and let $r_j = \mu_j^+/|\mu_j^-|$ denote the *hyperbolicity ratio.* We assume that

$$r_j \neq 1 : \quad j = 1, 2, 3. \tag{B.1}$$

Necessarily, $r_1 r_2 r_3 = 1$, by the quasi-Hamiltonian property of quadratic 3-cycles, so that without loss of generality $r_1 \leq r_2 \leq r_3$ and $r_1 < 1 < r_3$. We will treat the case $r_2 > 1$; the case $r_2 < 1$ is similar. That is:

$$r_1 < 1 < r_2 \leq r_3. \tag{B.2}$$

Consider an orbit Γ of (2.2) passing near U_j, as illustrated in Fig. B.1(b); define d to be the distance along $L_{j-1,j}$ between Γ and the unstable manifold coming into U_j, and define d' to be the distance along $L_{j,j+1}$ between Γ and the stable manifold leaving U_j. From the linearized description of the behavior close to U_j, we find that d and d' satisfy the asymptotic relation

$$d' \sim C_j d^{r_j}. \tag{B.3}$$

From (B.2)–(B.3), we immediately find that there exists a surface of curved saddle-saddle connections from U_j to U_{j+2} tangent to the 2-surface

$$d_{j+1,j+2} = -C_{j+1} d_{j,j+1}^{r_{j+1}}, \tag{B.4}$$

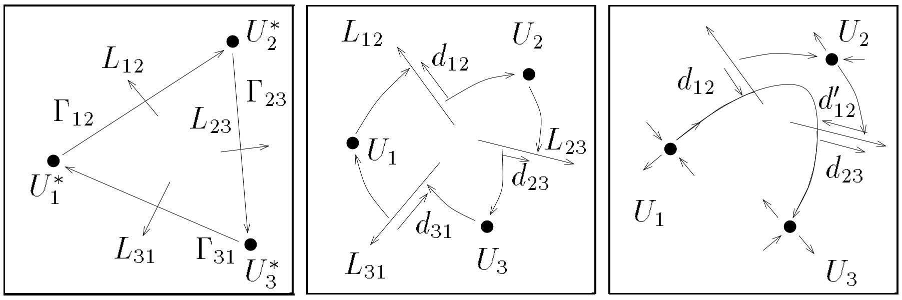

(a) A 3-cycle of shock waves

(b) Perturbed 3-cycle

(c) Curved saddle-saddle connection

Figure B.1: Phase portraits for the bifurcation of a 3-cycle of shock waves. In (c), $d_{12} < 0$, $d_{23} > 0$, and $d_{23} \sim -d'_{12} \sim -C_2 d_{12}^{r_2}$.

(see Fig. B.2(b)). This is in turn tangent to either $d_{j+1,j+2} = 0$ or $d_{j,j+1} = 0$, according as $r_{j+1} > 1$ or $r_{j+1} < 1$. In either case, the surface of curved connections from U_j to U_{j+2} is *transverse* to the surface of straight-line connections in the opposite sense, from $U_{j+2}$to U_j. Taking their intersections, we find that three different curves of 2-cycle connections emerge from the 3-cycle, connecting (U_1, U_3), (U_2, U_1), and (U_3, U_2). For the choices of r_j above, these are tangent to the coordinate axes $d_{23} = 0$, $d_{31} = 0$, and $d_{31} = 0$, respectively. For example, from (B.2)–(B.3), we find that there exists a surface of homoclinics $U_1 \to U_1$ tangent to the surface

$$d_{31} = 0. \qquad (B.5)$$

Homoclinic connections: Similarly (see Fig. B.2(a)), we find that there are three surfaces of homoclinic connections from U_j to itself, tangent to the surfaces

$$d_{j+2,j+3} = C_{j+2}[C_{j+1} d_{j,j+1}^{r_{j+1}} - d_{j+1,j+2}]^{r_{j+2}}, \qquad (B.6)$$

respectively. There are also various limit cycles, *etc.*, which we do not include. An abbreviated bifurcation diagram appears in Fig. B.1(c). Note that restricting to the (d_{23}, d_{31})-plane recovers essentially the two-saddle cycle bifurcation described in [5], Sections 3.3–3.4; more precisely, the portion of the three parameter bifurcation depicted here forms a cone over the two-parameter bifurcation described in the reference.

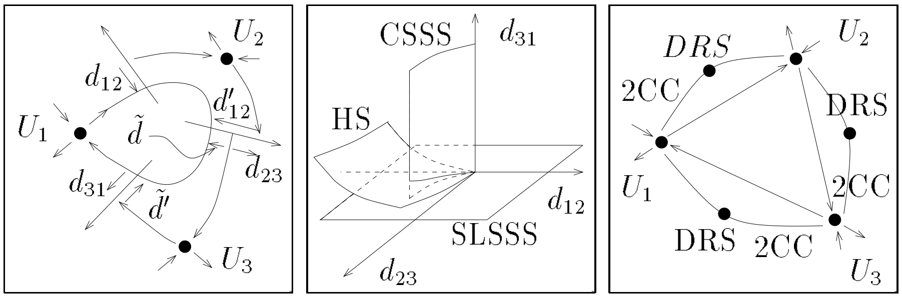

(a) Homoclinic orbit (b) Bifurcation diagram (c) Global structure

Figure B.2: The phase portrait for a homoclinic connection, the 3-parameter bifurcation diagram for a 3-cycle of shock waves, and the global structure of the 2-cycle curves in state space. In (a), $d_{12} < 0$, $d'_{12} \sim C_2 d_{12}^{r_2}$, $d_{23} > 0$, $\tilde{d} = d'_{12} - d_{23}$, $\tilde{d}' \sim C_3 \tilde{d}^{r_3}$, and $d_{31} > 0$. In (b), CSSS marks the surface of curved saddle-saddle connections from U_1 to U_3, SLSSS marks the surface of straight-line saddle-saddle connections U_3 to U_1, and HS marks the surface of homoclinic connections at U_1. In (c), 2CC marks the 2-saddle cycle curve.

Remark. Here we have assumed that Melnikov separations are related as depicted as in Figures B.1(c) and B.2(a). In general, there is a complicated case structure; see [5] for the analogous structure in 2-cycle bifurcation.

Summary: From each vertex of the 3-cycle there bifurcate two curves which are the locus of 2-cycles, together with the bifurcation diagrams associated to each separate 2-cycle. (See [5] for further description.)

B.1.1. Termination of the 2-cycle curve. We now discuss the behavior of the curve of 2-cycles as it leaves the vicinity of the 3-cycle. More generally, let us consider a general two-saddle cycle curve, possibly *not* connected to a 3-cycle vertex, and ask in what fashion this curve may terminate.

Local to *any* 2 saddle cycle, the set of 2 saddle cycles forms a one-parameter curve, so long as the surfaces of straight-line and curved transitional connections are transverse (*cf.* Ref [5]). We make the nondegeneracy assumption

(H1) Transversality is maintained at all 2 saddle cycles.

This property is difficult to verify for any particular model, but by dimensional considerations would appear to hold for generic choice of model parameters, the set of nontransverse cycles being codimension four (note: nontransversality in the three-parameter space (U_-, s) imposes two conditions). In addition, we point out that such transversality was observed numerically to hold for the example studied in [1] of Holden's model with viscosity $B = I$, hence should hold at least for models nearby this one; we point out that numerical studies of interest [16, 9] consider just such models.

Lemma B.1. *For a two-component quadratic flux model satisfying (H1), a 2-cycle curve extends until it terminates in one of six ways:*

(i) a third rest point (saddle) interrupts one of the saddle-saddle connections, forming a 3-cycle; or

(ii) a third rest point (node) combines with one of the saddles, changing the type of the connection to saddle-node/saddle, a degenerate, sonic *shock;*

(iii) the double cycle shrinks to a point (a DRS point, see [7]);

(iv) the curve forms a (nonterminating) loop.

(v) the curve approaches infinity.

(vi) the curve wanders indefinitely in a finite set, with ω-limit set (defined with respect to increasing arc length) consisting entirely of double-cycle bifurcation points (i)–(iii).

Remark. In (i), we allow the case that the third rest point be at infinity.

Proof: The two-saddle cycle curve continues locally by assumption of transversality (H1); thus, it either terminates at a bifurcation point or else continues globally. In the former case, continuous dependence dictates that the two-cycle in the limit either grows to infinity, (i), shrinks to a point, (iii), or else persists as a cycle that is not a two-saddle cycle. But, this implies either that one of the vertices collides with a second rest point to become a non-saddle, (ii), or else one or more new rest points interrupt the cycle. Since there remains always a node within the cycle [10, 11], and quadratic models have at most four rest points, two of which are accounted for at the (limits of the) original vertices, there can in fact be only one colliding/interrupting rest point. For the same reason, these must be of the types described (saddle, node, resp.), since otherwise there would have to be a third rest point involved in the collision

In the latter case, that the two-saddle cycle curve either goes to infinity, (v), or else wanders indefinitely within a finite set, the curve has a nontrivial ω-limit set (defined with respect to increasing arc length). But, the ω-limit, by continuous dependence, would also be a curve of 2-cycles, or possibly termination points as described above. Moreover, if it contains an ordinary 2-cycle point, then by local uniqueness, a consequence of transversality, (H1), the ω-limit set must agree with the two-saddle cycle curve, hence form a loop, (iv). The remaining possibility is (vi).

□

Now let us make the further assumption (again justified by codimension four violation):

(H2) All (codimension three) bifurcation points (i)–(iii) are nondegenerate.

We point out that in case (iii), (H2) has been shown to hold generically in [7]; a similar argument yields the result for case (i) (since the unique 3-cycle is determined by algebraic conditions, as the three DRS points of the reference). The precise configuration referred to in (ii) is a saddle-node to saddle double cycle, for which the connections at the saddle-node lie along the weak and strong saddles (a connection along the node direction would persist under perturbation, hence could not arise as the limit of two-saddle cycles).

Recall, further, that for quadratic flux models, depending on the behavior of the flux at infinity, each phase portrait (independent of U_-, s) contains four rest points in one of two configurations, either three saddles with a node contained in their convex hull (type I_B only), or else two nodes and two saddles, no one contained in the convex hull of the other three (all other types) (*cf.* Refs. [10, 11, 19]).

Theorem B.2. *For two-component Hurley-type quadratic flux models satisfying (H1)–(H2), only (i)–(iv) can occur; moreover, (i) occurs only for type I_B, (ii) never occurs for type I_B, and (iii) occurs only for type I_B–II_B models. In particular, for type I_B models, all two-saddle cycle curves either form isolated loops, or else connect DRS points to 3-cycle vertices; for type II_B models, all two-saddle cycle curves either form isolated loops, connect DRS points to sonic bifurcations points (ii), or else connect sonic bifurcation to sonic bifurcation points; for type III_B–IV_B models, two-saddle cycle curves either form loops or else connect sonic bifurcation to sonic bifurcation points.*

Remark. For quadratic flux models not of Hurley form, there may be the third possibility (v).

Proof: For a model of a given type only one of (i) or (ii) is possible. For, depending on the behavior of the flux at infinity, the phase portrait contains four rest points in one of two configurations, either three saddles with a node contained in their convex hull (Hurley type I_B only), or else two nodes and two saddles, no one contained in the convex hull of the other three (all other types) [10, 11, 19]. This configuration is independent of the choice of (U_-, s). In the first case, (ii) cannot occur unless (iii) in fact occurs. For, there is always a node contained in the interior of a 2-cycle [10, 11], so that two of the saddles would have to combine. Then, the three saddles would be colinear, and the node as well, being in their convex hull. But, a line containing three distinct rest points for a quadratic planar ODE must consist entirely of rest points, since a quadratic function with three zeroes is identically zero [10, 11], and thus *neither* endpoint of the 2-cycle can be a saddle. It follows that the node must combine with the remaining saddle, *i.e.*, the 2-cycle and all rest points must collapse to a single point, giving (iii). In the second case, clearly (i) cannot occur, since the only available rest points to interrupt the saddle-saddle connection is a node, which cannot lie on a cycle. Similarly, it was shown in [7] that DRS points occur only for models of type I_B–II_B, hence (iii) can occur only for such models. This verifies the statements about case structure for (i)–(iii).

By nondegeneracy assumption (H2), possibility (vi) is eliminated; for emerging from the nondegenerate bifurcation points of each of the types (i)–(iii) are *locally unique* curves of two-saddle cycles, hence again the ω-limit set would have to agree with the two-saddle cycle curve itself, and the latter would terminate in one of cases (i)–(iii).

Remark. For bifurcation for the saddle-node/saddle cycle, case (ii) above, this fact can be deduced using the techniques of [25, 26]; for cases (i) and (iii), the bifurcations are given in B.1 above and in [7], respectively.

Finally, case (v) is disallowed by the result of Freistühler and Zumbrun [15] that, for Hurley type models, curved shock profiles occur only on a bounded subdomain of the state space. Since straight line profiles have a unique sense, this immediately implies that double-saddle connections cannot occur outside this set.

Now restrict to cases I_B–II_B:

We first show that a two-saddle cycle curve emerging from a 3-cycle cannot terminate at a 3-cycle, and similarly a two-saddle cycle curve emerging from a DRS point cannot terminate at a DRS point. For quadratic flux models, it is easily seen that the first situation is impossible, by properties of straight line connections. For, there is a unique vertex with straight line connection leaving in a certain direction. Since the direction of the straight line connections is constant along the 2-cycle curve, we find that the curve cannot strike a second vertex of the 3-cycle. Moreover, it cannot return to the same vertex, since it would have to enter along the curve for which the straight line connection occurs in a different direction.

Similarly, a 2-cycle emerging from a DRS point cannot terminate at a DRS point. For, the endpoints of straight line connections in a certain direction lie on opposite sides of a given line, specifically, the *viscosity line* described in Theorem . Those which are transitional lie additionally in a "sonic wedge" intersecting the viscosity line at a single point [22]. Thus there is a unique DRS point with straight line connections in a given direction. Again noting that the direction of the straight line connections is constant along the 2-cycle curve, we find that it cannot terminate at a different DRS point. Moreover, as above, it cannot terminate at the same DRS point, since it would have to enter along the direction in which the straight line connection proceeds in opposite sense from the point U_-. Combining, we see that (i) and (iii) can occur at most once apiece for each single 2-cycle curve.

Thus we see that for type I_B Hurley models, each (terminating, *i.e.*, non-loop) 2-cycle curve must extend precisely from a 3-cycle vertex to a DRS point. For type II_B Hurley models, the 2-cycle curve emerging from a DRS point ends instead at a sonic degeneracy (possibility (ii)), while 3-cycles do not exist; we do not know in this case whether a 2-cycle curve may connect two sonic degeneracies, but a priori we must admit this possibility. Recall (above) that type III_B–IV_B models do not have saddle connections near the DRS point, nor do they possess 3-cycles. If they have 2-cycles, then, these must be of a type connecting sonic degeneracies.

□

B.2. Global Structure. For Hurley type models of Case I_B, we thus have the "typical" figure 2(c), which, provided that the Melnikov integrals for 2-cycles never vanish (a nondegeneracy condition that is apparently difficult to check), of a 3-cycle, with vertices connected by two-saddle cycle curves to three DRS points. Thus we obtain almost all of the same structure discovered by Azevedo in the special case of Holden's model [1], [4]. For this model, we point out that it is easy to generate explicitly a variety of multi-loop solutions, which are found numerically to indeed be long-lasting. The systematic investigation of the general case we leave for the future.

Remark. In principle, all information up to first order about homoclinic and transitional maps can be found near the triple cycle, using methods similar to those of [5]: namely, we can use the linearized Hugoniot relation together with our knowledge of the straight line maps to explicitly calculate all quantities of interest. Likewise, such information can be found near the DRS points using the corresponding results of [14] and undoing the coordinate changes used in [7] to reduce to their normal form. As seen in [5], such information is useful in constructing Riemann solutions.

References

[1] Azevedo, A., *Soluções Fundamentais Múltiplas em Sistemas de Leis de Conservação Hiperbólico–Elíticos*, Pontifícia Universidade Católica do Rio de Janeiro, Ph.D. Thesis, in Portuguese, Rio de Janeiro, Brazil, (1991).

[2] Azevedo, A.; Marchesin, D., *Multiple Viscous Profile Riemann Solutions in Mixed Elliptic-Hyperbolic Models for Flow in Porous Media*, In B. Keyfitz and M. Shearer, editors, *Hyperbolic Equations that Change Type*, Vol. 27 of IMA Volumes in Mathematics and its Applications, Springer-Verlag, New York–Heidelberg–Berlin, (1990), 1–17.

[3] Azevedo, A.; Marchesin, D., *Multiple Viscous Solutions for Systems of Conservation Laws*, Trans. Amer. Math. Soc., Vol. 347, (1995) 3061–3078.

[4] Azevedo, A.; Marchesin, D., *The manifold of quasi-Riemann solutions*, in preparation, (1999)

[5] Azevedo, A.; Marchesin, D.; Plohr, B.; Zumbrun, K., *Nonuniqueness of Nonclassical Solutions of Riemann Problems*, Z. Angew. Math. Phys., Vol. 47, (1996), 977–998.

[6] Azevedo, A.; Marchesin, D.; Plohr, B.; Zumbrun, K., *Nonuniqueness of Solutions of Riemann Problems Caused by* 2*-Cycles of Shock Waves*, In *Hyperbolic Problems: Theory, Numerics, Applications (Stony Brook, NY, 1994)*, World Scientific, River Edge, NJ, (1996), 43–51.

[7] Azevedo, A.; Marchesin, D.; Plohr, B.; Zumbrun, K., *Bifurcation of nonclassical viscous shocks profiles from the constant state*, Comm. Math. Phys., Vol. 202, (1999), 267–290.

[8] Cairo, L.; Llibre, J., *Integrability and algebraic solutions for planar polynomial differential systems with emphasis on the quadratic systems*, IME/USP (Universidade de São Paulo, Brazil) Report No., 2, (1999).

[9] Čanić, S.; Peters, G., *Nonexistence of Riemann Solutions and Majda-Pego Instability*, J. Differential Equations, (1998), submitted.

[10] Chicone, C., *Quadratic gradients on the plane are generically Morse-Smale*, J. Differential Equations, Vol. 33 (2), (1979), 159–166.

[11] Chicone, C., On bifurcation of limit cycles from centers, I n J.-P. Françoise and R. Roussarie, editors, *Bifurcations of Planar Vector Fields (Luminy, 1989)*, Vol. 1455, Lect. Notes Math., Springer-Verlag, New York–Heidelberg–Berlin, (1990), 20–43.

[12] Courant,; Friedrichs, K., *Supersonic Flow and Shock Waves*, Springer-Verlag, New York, (1976).

[13] Dumortier, F.; Roussarie, R.; Sotomayor, J., *Generic 3-Parameter Families of Vector Fields on a Plane, Unfolding a Singularity with Nilpotent Linear Part. The Cusp Case of Codimension 3.*, Ergodic Theory and Dynamical Systems, Vol. 7, (1987), 375–413.

[14] Dumortier, F.; Roussarie, R.; Sotomayor, J.; Żoładek, H., *Nilpotent Singularities and Abelian Integrals*, Lect. Notes Math., Vol. 1480 , Springer-Verlag, New York–Heidelberg–Berlin, (1991).

[15] Freistühler, H.; Zumbrun, K., *Private communication*, (1997).

[16] Frid, H.; Liu, I. S., *Oscillation Waves in Riemann Problems inside Elliptic Regions for Conservation Laws of Mixed Type*, Z. angew. Math. Phys., Vol. 46, (1995), 913–931.

[17] Gardner, R. A.; Zumbrun, K., *The gap lemma and geometric criteria for instability of viscous shock profiles*, Comm. Pure Appl. Math., Vol. 51 (7), (1998), 797–855.

[18] Gel'Fand, I. M., *Some Problems in Theory of Quasilinear Equations*, Amer. Mat. Soc. Trans., ser. 2, Vol. 29, (1963), 295–381. English transl.

[19] Gomes, M. E., *Problema de Riemann singular para um modelo de quarta ordem em escoamento multifásico*, Pontifícia Universidade Católica do Rio de Janeiro, Ph.D. Thesis, in Portuguese, Rio de Janeiro, Brazil, (1987).

[20] Guckenheimer, J.; Holmes, P., *Nonlinear Oscillations, Dynamical Systems, and Bifurcations of Vector Fields*, Springer-Verlag, New York–Heidelberg–Berlin, (1986).

[21] Hurley, J., *Effects of Viscous Terms on Solutions of Riemann Problems*, State Univ. of New York at Stony Brook, Ph.D. Thesis, (1995).

[22] Isaacson, E.; Marchesin, D.; Plohr, B., *Transitional Waves for Conservation Laws*, SIAM J. Math. Anal., Vol. 21, (1990), 837–866.

[23] Mourtada, A., *Cyclicité finie des Polycycles Hyperboliques de Champs de Vecteurs du Plan Mise sous Forme Normale*, In J.-P. Françoise and R. Roussarie, editors, *Bifurcations of Planar Vector Fields (Luminy, 1989)*, Vol. 1455, Lect. Notes Math., Springer-Verlag, New York–Heidelberg–Berlin, (1990), 272–314.

[24] Schaeffer, D.; Shearer, M., *Riemann Problems for Nonstrictly Hyperbolic* 2×2 *Systems of Conservation Laws*, Trans. Amer. Math. Soc., Vol. 304, (1987), 267–306.

[25] Schecter, S., *The Saddle-Node Separatrix-Loop Bifurcation*, SIAM J. Math. Anal., Vol. 18, (1987), 1142–1156.

[26] Schecter, S., *Simultaneous Equilibrium and Heteroclinic Bifurcation of Planar Vector Fields via the Mel'nikov Integral*, Nonlinearity, Vol. 3, (1990), 79–99.

[27] Wenstrom, J.; Plohr, B., *The Effects of Viscous Terms on Riemann Problem Solutions for Quadratic Conservation Laws*, Report No., SUNYSB-AMS-00-23, State University of New York at Stony Brook, (2000).

[28] Żoładek, H., *The Cyclicity of Triangles and Segments in Quadratic Systems*, J. Differential Equations, Vol. 122, (1995), 137–159.

Departamento de Matemática
Universidade de Brasília
70910-900 Brasília, DF, Brazil
e-mail: arthur@mat.unb.br

Instituto de Matemática Pura e Aplicada
Estrada Dona Castorina 110
22460-320 Rio de Janeiro, RJ, Brazil
e-mail: marchesi@impa.br

Departments of Mathematics and of
Applied Mathematics and Statistics
State University of New York
at Stony Brook
Stony Brook, NY 11794-3651
e-mail: plohr@ams.sunysb.edu

Department of Mathematics
Indiana University
Bloomington, IN 47405
e-mail: kzumbrun@ucs.indiana.edu